

Feasibility, tailoring and properties of polyurethane/bioactive glass composite scaffolds for tissue engineering

Francesco Baino · Enrica Verné ·
Chiara Vitale-Brovarone

Received: 21 January 2009 / Accepted: 19 May 2009 / Published online: 2 June 2009
© Springer Science+Business Media, LLC 2009

Abstract This research work aims to propose highly porous polymer/bioactive glass composites as potential scaffolds for hard-tissue and soft-tissue engineering. The scaffolds were prepared by impregnating an open-cells polyurethane sponge with melt-derived particles of a bioactive glass belonging to the $\text{SiO}_2\text{-P}_2\text{O}_5\text{-CaO-MgO-Na}_2\text{O-K}_2\text{O}$ system (CEL2). Both the starting materials and the composite scaffolds were investigated from a morphological and structural viewpoint by X-ray diffraction analysis and scanning electron microscopy. Tensile mechanical tests, carried out according to international ISO and ASTM standards, were performed by using properly tailored specimens. In vitro tests by soaking the scaffolds in simulated body fluid (SBF) were also carried out to assess the bioactivity of the porous composites. It was found that the composite scaffolds were highly bioactive as after 7 days of soaking in SBF a HA layer grew on their surface. The obtained polyurethane/CEL2 composite scaffolds are promising candidates for tissue engineering applications.

1 Introduction

Tissue engineering represents a promising approach to repair and regenerate a wide variety of damaged human tissues, avoiding the problems involved in transplantation [1]. Autografts have been commonly considered the “gold standard” in bone reconstructive surgery, but their

availability is limited and harvesting the patient’s own tissue can cause death of healthy tissue at the donor site. Allografts are in larger supply but carry the risks of pathologic transmission. The use of man-made alloplastic materials overcomes the drawbacks related to autografts and allografts and, in addition, avoids the need for a permanent implant.

Different natural and synthetic materials have been widely investigated to produce tissue engineering scaffolds, i.e. usually porous implants acting as 3-D templates for cells adhesion, growth and proliferation.

Biocompatible polymers, such as degradable polylactide, polyglycolide and their co-polymers, are the most promising candidates for soft-tissue engineering applications [2, 3].

As regards hard-tissue engineering, bioceramics have been proposed as bone graft materials for many decades and they have a range of applications including bone defects filling, fracture fixation, trauma and tumours treatment, maxillofacial and spinal surgery [4–8]. Hydroxyapatite (HA) has been traditionally used for hard-tissue repair because of its chemical and crystallographic similarity to the carbonated apatite in human teeth and bone [9]. Calcium-phosphate (CaP) salts have usually been adopted as fillers for small bone cavities in orthopaedics and in restorative dentistry [10, 11]. Bioactive glasses (BGs) and glass-ceramics (BGCs), basically composed of SiO_2 , P_2O_5 , Na_2O and CaO , have been investigated due to their highly bioactive behaviour [12–14]. Above the traditional silica-based BGs, phosphate-based scaffolds, able to resorb at the same time as the bone is repaired, have been recently proposed [15, 16].

In previous years, polymer/ceramic (glass) porous composites have attracted increasing interest as scaffolds for bone tissue engineering. Specifically, two classes of composite scaffolds have been fabricated and investigated: (i) polymer-based scaffolds coated with ceramic (glass) particles and (ii) polymer-coated ceramic (glass) scaffolds.

F. Baino (✉) · E. Verné · C. Vitale-Brovarone
Materials Science and Chemical Engineering Department,
Politecnico di Torino, Corso Duca degli Abruzzi 24,
10129 Torino, Italy
e-mail: francesco.baino@polito.it

As examples of the type (i), PLGA/amorphous CaP, PLLA/HA and PLGA/Bioglass[®] composite scaffolds have been proposed for bone regeneration [17–19]. The ceramic (glass) particles were added to the polymer to enhance scaffold bioactivity, aiming to induce implant mineralization/osteointegration.

In the case (ii), the polymer was introduced to strengthen the ceramic (glass) scaffold structure: the polymer layer acted as a glue, holding the glass particles together as the struts start to fail [20].

Polymer/ceramic (glass) scaffolds have been mainly proposed for hard-tissue engineering but some studies, involving the use of such scaffolds for soft-tissue regeneration, have been also carried out. For instance, PDLA/Bioglass[®] composite scaffolds have been investigated for lung tissue engineering [21].

Concerning the composite scaffolds fabricated by using a polymer and, specifically, bioactive glass particles, in the authors' knowledge a wide range of polymers has been tested but only Bioglass[®] powders [22] have been adopted as inorganic phase. This research work pursued the aim to fabricate polyurethane-based composite scaffolds coated with melt-derived particles of a bioactive glass (CEL2) different from Bioglass[®]. The prepared scaffolds were characterized in terms of structure, morphology and in vitro bioactivity. In addition, mechanical tests were carried out on “dumbbell-shaped” specimens apt for tensile strength tests according to international standards. In fact, specific ASTM and ISO standards [23, 24] are recommended for tensile tests on biomaterials [25], but at present only one study was carried out to assess the tensile strength of polymer/glass composite scaffolds [26], due to the difficulties occurring in the shaping of specimens.

2 Materials and methods

2.1 Starting materials

The polymeric skeleton of the composite scaffolds was a commercial polyurethane (PU) open-cell sponge (density $\sim 20 \text{ kg m}^{-3}$) characterized by a 3-D network of macropores.

The glass particles necessary for polymer coating were produced by a traditional melting/quenching route. Briefly, the silica-based glass (CEL2; molar composition: 45% SiO₂, 3% P₂O₅, 26% CaO, 7% MgO, 15% Na₂O, 4% K₂O [27]) was synthesized by melting the reagents, i.e. SiO₂, Ca₃(PO₄)₂, CaCO₃, (MgCO₃)₄ · Mg(OH)₂ · 5H₂O, Na₂CO₃ and K₂CO₃, in a platinum crucible in air at 1400°C for 1 h (heating rate: 5°C min⁻¹) to ensure homogeneity and by then quenching the melt in cold water. The so-obtained “frit” was ground by ball milling and carefully sieved to

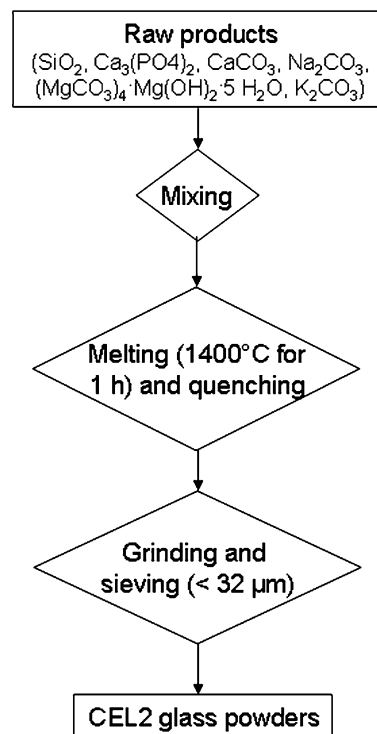


Fig. 1 Flow-chart of glass synthesis

obtain particles with diameter below 32 μm. The steps involved in glass synthesis are resumed in Fig. 1.

The glass powders were analyzed by means of wide-angle (2θ within 10–60°) X-ray diffraction (XRD) by using a X'Pert Philips diffractometer (Cu anode with K α radiation, incident wavelength $\lambda = 1.5405 \text{ \AA}$, Bragg-Brentano geometry) operating at 40 kV and 30 mA, with a step size $\Delta(2\theta) = 0.02^\circ$ and a fixed counting time of 1 s per step.

Scanning electron microscopy (SEM, Philips 525 M operating at 15 kV) was carried out on both the CEL2 particles and the PU sponge.

2.2 Scaffolds fabrication

The PU sponge was carefully shaped to obtain two kinds of samples: (i) 15.0 × 15.0 × 15.0 mm³ cubic blocks and (ii) “dumbbell-shaped” specimens necessary for mechanical tests. The so-tailored bare polymer underwent a process of infiltration by dipping in a water-based CEL2 slurry to finally obtain PU/CEL2 composite scaffolds. The weight ratio of slurry components was set as follows: 30% CEL2, 6% polyvinyl alcohol (PVA), 64% water. PVA was used as binding agent so that the glass particles adhere to the surfaces of the polymer. After PVA hydrolysis at 60°C for 1 h under magnetic continuous stirring, CEL2 powders were added to the solution. After slurry mixing at room temperature (RT) for 0.5 h, the bare PU samples were soaked

for 30 s in the slurry which infiltrates the polymer structure; the samples were then extracted and the exceeding slurry was removed by pressing (20 kPa for 1 s). The process was repeated for four times to obtain a continuous and homogeneous glass coating on the polymeric structure; finally, the resulting composite scaffolds were dried at room temperature on glass plates.

The stages necessary for composite scaffolds fabrication are resumed in Fig. 2.

2.3 Scaffolds characterization

The PU/CEL2 composite scaffolds were investigated by SEM in order to evaluate the results of the fabrication process.

The porous content of the bare sponge and of the composite scaffolds was easily assessed from the mass and

dimensions of the samples. Specifically, the composite scaffolds were weighted before and after the glass infiltration process; the porosity P (vol.%), i.e. the void space in the scaffold volume, was finally calculated as [28]:

$$P = \left(1 - \frac{\rho_s}{\rho_0}\right) \cdot 100,$$

where ρ_s is the apparent density of the scaffold and ρ_0 is the density of the material of which the scaffold is fabricated. Named m_p the mass of the bare polymer, m_g the mass of the infiltrated glass, φ_p the mass fraction of PU, φ_g the mass fraction of glass and V the scaffold volume, the apparent density of the composite scaffold can be calculated as $\rho_s = \varphi_p \frac{m_p}{V} + \varphi_g \frac{m_g}{V}$. The density of non-porous material was determined as $\rho_0 = \varphi_p \rho_p + \varphi_g \rho_g$, where ρ_p and ρ_g are the densities of PU and CEL2, respectively.

The “dumbbell-shaped” scaffolds underwent tensile strength tests, that were performed by using a MTS System Corp. apparatus (cross-head speed set at 10 mm min^{-1}). The failure tensile stress σ_t (MPa) was obtained as

$$\sigma_t = \frac{F_b}{S},$$

where F_b (N) is the tensile load at break and S (mm^2) is the resistant cross-section perpendicular to the load axis.

The Young’s modulus E (MPa) was calculated from the Hookean region of the stress–strain plot.

The energy absorbed per unit volume $W_{0 \rightarrow \varepsilon^*}$ (J cm^{-3}) by the scaffold was defined as the energy necessary to deform a specimen from the unloaded condition ($\sigma = 0$, $\varepsilon = 0$) to a strain ε^* (breaking off) and was calculated as the area under the stress–strain curve up to ε^* [29]:

$$W_{0 \rightarrow \varepsilon^*} = \int_0^{\varepsilon^*} \sigma(\varepsilon) d\varepsilon.$$

In vitro bioactivity was investigated by soaking $15.0 \times 15.0 \times 15.0 \text{ mm}^3$ composite scaffolds for 7 days in 30 ml of acellular simulated body fluid (SBF) maintained at controlled temperature (37°C), as described by Kokubo’s protocol [30]. The solution was replaced twice a week to approximately simulate fluid circulation in the human body. The samples were analyzed by SEM and EDS (EDAX Philips 9100) analysis to assess the precipitation of apatite-like phases.

3 Results and discussion

3.1 Morphological and structural investigations

The morphology of CEL2 particles used to coat the PU sponge is non-spherical, irregular and angular, as shown in

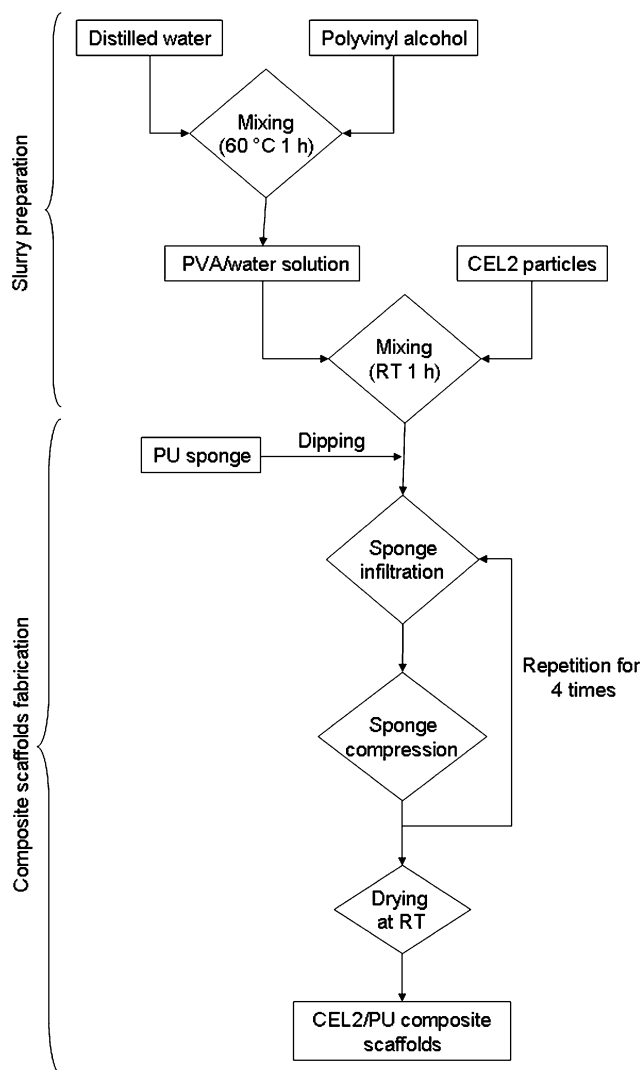


Fig. 2 Flow-chart of sponge-impregnation method for fabrication of composite scaffolds

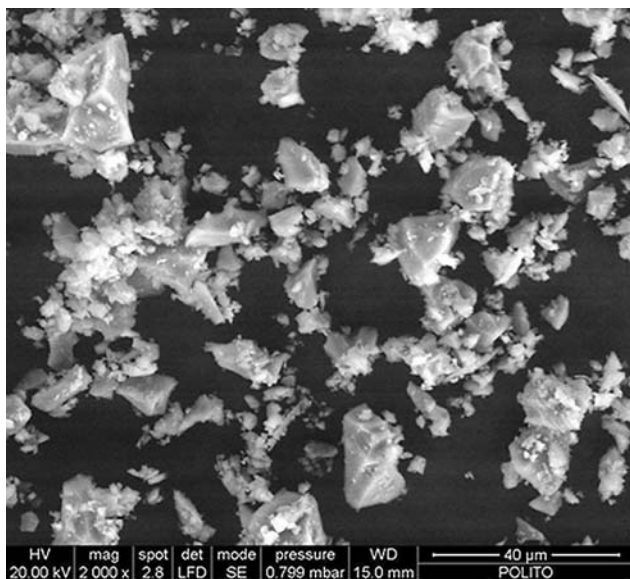


Fig. 3 Low-magnification SEM micrograph of glass particles used for PU sponge coating

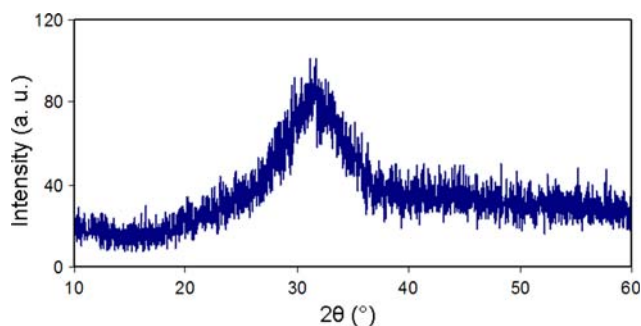


Fig. 4 XRD pattern of CEL2 particles

Fig. 3. In addition, a bimodal distribution of particles size can be observed: (i) particles ranging within 20–30 μm and (ii) particles with size below 10 μm .

The glassy nature of CEL2 particles was demonstrated by XRD investigations, as the broad halo depicted in **Fig. 4** reveals that the material was completely amorphous.

Low-magnification SEM observations confirmed that the bare PU sponge exhibited a 3-D network of highly interconnected macropores ranging within 200–800 μm , as shown in **Fig. 5**. After polymer impregnation, a continuous and uniform CEL2 particles coating was successfully obtained on sponge trabeculae (**Fig. 6**). Some clotted pores are visible, but, in general, the pores remain—at least partially—open and interconnected.

The sponge-impregnation method used for the fabrication of the composite scaffolds involves a remarkable potential for reconstructive surgery due to two reasons: (i) grafts of various size and shape can be easily tailored to each single patient and (ii) the problem of controlling the

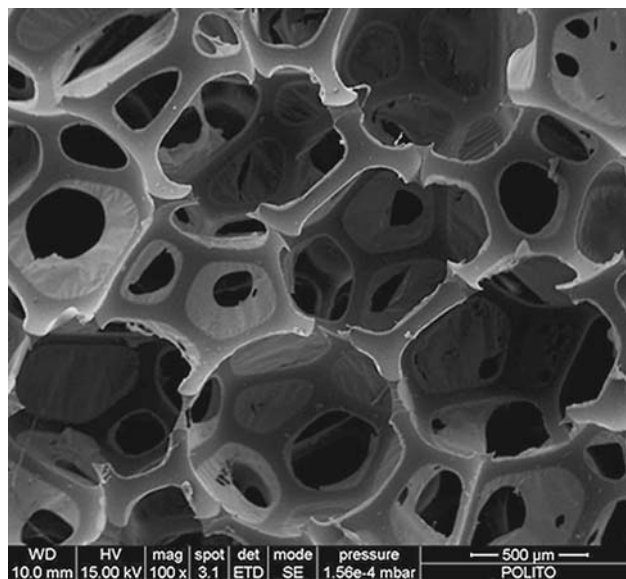


Fig. 5 Structure of the bare polyurethane sponge

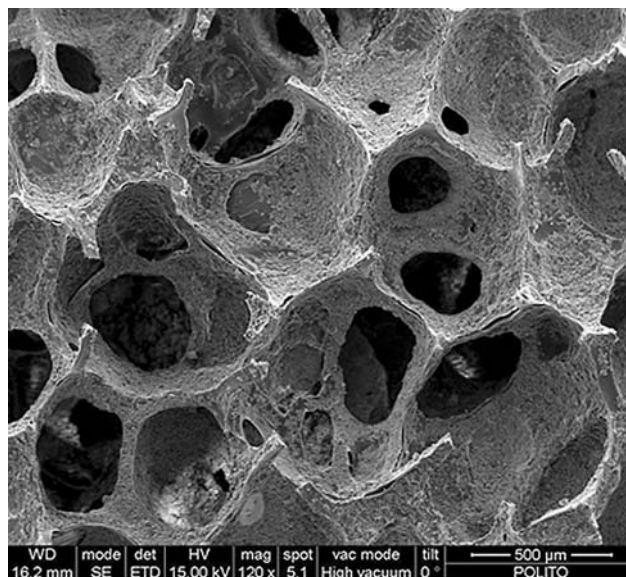


Fig. 6 Morphology of the composite scaffold

volumetric shrinkage which occurs in ceramic (glass) scaffolds is successfully overcome.

The porous content of PU/CEL2 scaffolds is close to that of the bare sponge (**Table 1**), demonstrating that the glass coating does not significantly reduce the pores size, as already shown by SEM observations (**Fig. 6**).

3.2 Mechanical characterization

Figure 7a shows a “dumbbell-shaped” scaffold used for tensile strength tests; two examples of tensile stress–strain curves (bare polymer and composite) are depicted in **Fig. 7b**.

Table 1 Samples porosity assessed via density measurements^a

Sample	<i>P</i> (vol.%)
Bare sponge	95.0 ± 4.0
Composite scaffold	87.0 ± 8.0

^a Five samples tested for each type

For both samples, the plots show an initial Hookean region (positive slope) in which stress increases in proportion to strain (elastic behaviour), followed by plastic behaviour (a plateau region is evident in (2)) and, finally, by a failure region ending with the specimen breaking off.

The mechanical properties inferred from the stress–strain curves are resumed in Table 2. A low standard deviation was assessed for these data, thus confirming that a good reproducibility of the specimens was achieved.

No statistically significant differences in terms of failure strength can be observed between bare sponge and composite scaffold.

The elastic modulus of the porous composites is one order of magnitude higher than bare sponge because, as expected, the glass coating increases the scaffold stiffness. In addition, the composite scaffolds showed limited energy absorption until failure in comparison with the bare polymer.

With regard to scaffolds mechanical properties, polymer/ceramic (glass) composite scaffolds have been proposed by many authors for hard-tissue substitution [17–20, 27, 31], but it should be noticed that the elastic stiffness and the mechanical strength of today’s available polymer/ceramic (glass) composite scaffolds, including those prepared in the present work, are inadequate if compared to the tissues they should temporarily replace. This drawback is particularly evident for implants devoted to bone substitution because polymer/glass porous composites are at least one order of magnitude weaker than natural cancellous bone [32], and they could successfully replace bone

Table 2 Mechanical properties of the scaffolds^a

Sample	<i>E</i> (MPa)	σ_r (MPa)	$W_{0 \rightarrow \epsilon^*}$ (J cm ⁻³)
Bare sponge	0.12 ± 0.020	0.12 ± 0.010	0.15 ± 0.025
Composite scaffold	1.35 ± 0.050	0.10 ± 0.020	0.037 ± 0.010

^a Five samples tested for each type

portions only after careful optimizations to reach a significant improvement of the mechanical properties. Although the composite scaffolds prepared in this research work exhibit not satisfactory mechanical features and, therefore, their potential use at present may be limited by such drawback, however they are interesting for tissue regeneration applications thanks to (i) the easiness of samples shaping according to the patient’s need and (ii) their excellent bioactivity, as demonstrated in the Sect. 3.3. Applications for bone substitution can be suggested, as proposed by other authors for Bioglass[®]-coated polymeric scaffolds [20, 33]. It should be noticed that, in this case, the replacement of strictly non-bearing bone portions is recommended.

3.3 In vitro bioactivity assessment

Figure 8a shows that globe-shaped agglomerates, resembling the typical “cauliflower morphology” of hydroxyapatite (HA), are well distinguishable on scaffold surface after 7 days of soaking in SBF. The glass particles lie underneath the newly formed layer. EDS analysis, reported in Fig. 8b, confirms that the newly formed phase is HA, because it exhibits a Ca/P molar ratio (~1.66) which closely approaches the natural HA stoichiometric value (Ca/P = 1.67). The presence of a weak peak for silicon (Si) can be attributed to the underlying silica-rich gel layer, due to the bioactive process as described by Hench [12]. The peak of silver (Ag) is due to the metal coating necessary for analysis.

Fig. 7 Tensile strength tests: **a** “dumbbell-shaped” bare sponge specimen; **b** typical stress–strain curves of (1) bare sponge and (2) composite scaffold

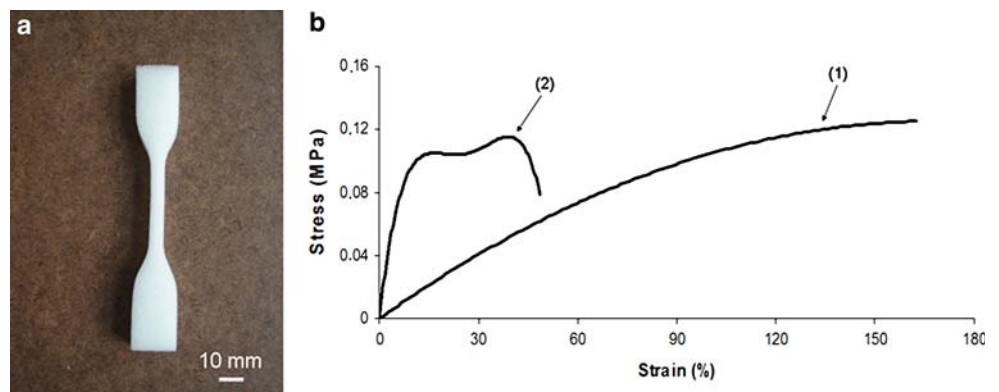
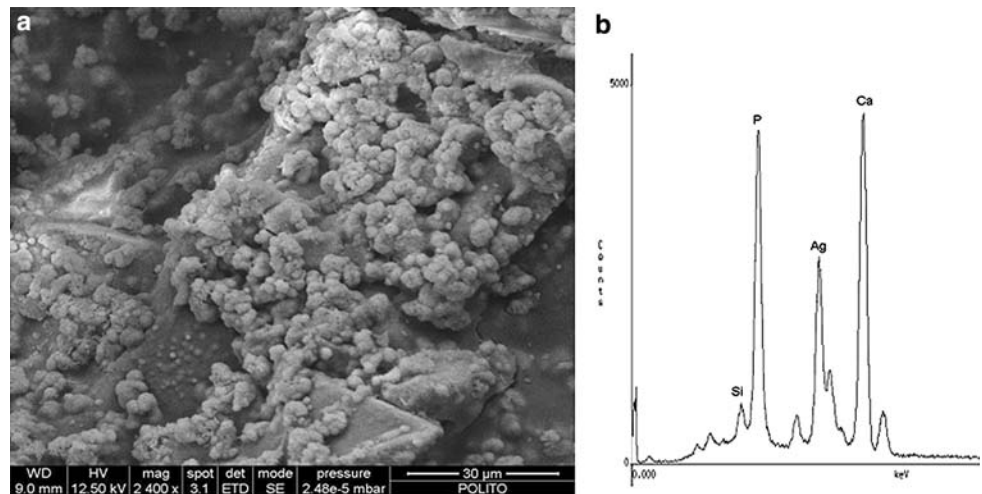


Fig. 8 In vitro bioactivity tests: **a** scaffold surface after 7 days of soaking in SBF and **b** corresponding EDS pattern



The sponge polymer (polyurethane) is biocompatible [34] and, as expected, does not affect the bioactivity of CEL2 particles. The in vitro behaviour of the composite scaffolds is similar to that shown by the only CEL2 [27], because the formation of a HA layer in both cases.

The pH variations induced by the scaffold soaked in SBF are quite moderate (pH = 8.20 after soaking for 24 h and pH = 7.80 after soaking for 7 days were registered, with respect to pH = 7.40 of the as-prepared SBF), thus no cytotoxic effect is foreseen after in vivo implantation.

4 Conclusions

In this research work 3-D foam-like polyurethane/bioactive glass composite scaffolds were produced by the sponge-impregnation technique. Specifically, macroporous polyurethane-based scaffolds coated with a continuous and homogeneous CEL2 layer were successfully obtained. The scaffolds were tailored in form of “dumbbell-shaped” specimens apt to carry out tensile strength tests according to ASTM and ISO standards; in this sense, the present work is a preliminary study about tensile behaviour of potential composite substitutes for tissue engineering.

The mechanical properties of the obtained porous composites were comparable to those of today’s available similar scaffolds proposed for hard-tissue and soft-tissue engineering. In addition, the prepared scaffolds showed an excellent bioactive behaviour. In fact, the in vitro studies showed that the CEL2 coating imparted high bioactivity to the scaffolds by promoting the formation of a hydroxyapatite layer on their surface.

Therefore, the prepared scaffolds are interesting candidates for tissue engineering applications due to their easiness of fabrication and bioactive properties.

Acknowledgements The authors gratefully acknowledge the financial support of Regione Piemonte (Ricerca Sanitaria Finalizzata) supplied for this work.

References

- Schlickewei W, Schlickewei S. The use of bone substitutes in the treatment of bone defects—the clinical view and history. *Macromol Symp.* 2007;253:10–23. doi:10.1002/masy.200750702.
- Wu L, Ding J. In vitro degradation of three-dimensional porous poly(D,L -lactide-co-glycolide) scaffolds for tissue engineering. *Biomaterials.* 2004;25:5821–30. doi:10.1016/j.biomaterials.2004.01.038.
- Lin ASP, Barrows TH, Cartmell SH, Guldberg RE. Microarchitectural and mechanical characterization of oriented porous polymer scaffolds. *Biomaterials.* 2003;24:481–9. doi:10.1016/S0142-9612(02)00361-7.
- Wolff D, Goldberg VM, Stevenson S. Histomorphometric analysis of the repair of a segmental diaphyseal defect with ceramic and titanium fibermetal implants: effects of bone marrow. *J Orthop Res.* 1994;12:439–46. doi:10.1002/jor.1100120317.
- Kon E, et al. Autologous bone marrow stromal cells loaded onto porous hydroxyapatite ceramic accelerate bone repair in critical-size defects of sheep long bones. *J Biomed Mater Res.* 2000;49:328–37. doi:10.1002/(SICI)1097-4636(20000305)49:3<328::AID-JBM5>3.0.CO;2-Q.
- Fredericks DC, et al. Segmental bone defect repair using sintered, porous ceramics. *Key Eng Mater.* 2002;218–220:409–12. doi:10.4028/www.scientific.net/KEM.218-220.409.
- Wilson CE, et al. A new in vivo screening model for posterior spinal bone formation: comparison of ten calcium phosphate ceramic material treatments. *Biomaterials.* 2002;27:302–14. doi:10.1016/j.biomaterials.2005.06.041.
- Marcacci M, et al. Stem cells associated with macroporous bioceramics for long bone repair: 6- to 7-year outcome of a pilot clinical study. *Tissue Eng.* 2007;13:947–55. doi:10.1089/ten.2006.0271.
- Ozawa N, Negami S, Odaka T, Morii T, Koshino T. Histological observations on tissue reaction of the rat calcaneal tendon to sintered hydroxyapatite. *J Mater Sci Lett.* 1989;8:869–71. doi:10.1007/BF01729929.
- LeGeros RZ. Biodegradation and bioresorption of calcium phosphate ceramics. *Clin Mater.* 1993;14:65–88. doi:10.1016/0267-6605(93)90049-D.

11. LeGeros RZ, Lin S, Rohanzadeh R, Mijares D, LeGeros JP. Biphasic calcium phosphate bioceramics: preparation, properties and applications. *J Mater Sci: Mater Med*. 2003;14:201–9. doi:[10.1023/A:1022872421333](https://doi.org/10.1023/A:1022872421333).
12. Hench LL. Bioactive materials: the potential for tissue regeneration. *J Biomed Mater Res*. 1998;41:511–8. doi:[10.1002/\(SICI\)1097-4636\(19980915\)41:4<511::AID-JBM1>3.0.CO;2-F](https://doi.org/10.1002/(SICI)1097-4636(19980915)41:4<511::AID-JBM1>3.0.CO;2-F).
13. Hench LL. Biomaterials: a forecast for the future. *Biomaterials*. 1998;19:1419–23. doi:[10.1016/S0142-9612\(98\)00133-1](https://doi.org/10.1016/S0142-9612(98)00133-1).
14. Jones JR, Ehrenfried LM, Hench LL. Optimising bioactive glass scaffolds for bone tissue engineering. *Biomaterials*. 2006;27:964–73. doi:[10.1016/j.biomaterials.2005.07.017](https://doi.org/10.1016/j.biomaterials.2005.07.017).
15. Knowles JC. Phosphate based glasses for biomedical applications. *J Mater Chem*. 2003;13:2395–401. doi:[10.1039/b307119g](https://doi.org/10.1039/b307119g).
16. Abou EA, Knowles JC. Physical and biocompatibility studies of novel titanium dioxide doped phosphate-based glasses for bone tissue engineering applications. *J Mater Sci: Mater Med*. 2008;19:377–86. doi:[10.1007/s10856-007-3079-5](https://doi.org/10.1007/s10856-007-3079-5).
17. Khan YM, Katti DS, Laurencin CT. Novel polymer-synthesized ceramic composite-based system for bone repair: an in vitro evaluation. *J Biomed Mater Res A*. 2004;69:728–37.
18. Zhang RY, Ma PX. Poly(-hydroxyl acids)/hydroxyapatite porous composites for bone-tissue engineering. I. Preparation and morphology. *J Biomed Mater Res*. 1999;44:446–55. doi:[10.1002/\(SICI\)1097-4636\(19990315\)44:4<446::AID-JBM11>3.0.CO;2-F](https://doi.org/10.1002/(SICI)1097-4636(19990315)44:4<446::AID-JBM11>3.0.CO;2-F).
19. Stamboulis AG, Hench LL, Boccaccini AR. Mechanical properties of biodegradable polymer sutures coated with bioactive glass. *J Mater Sci: Mater Med*. 2002;4:843–8. doi:[10.1023/A:1016544211478](https://doi.org/10.1023/A:1016544211478).
20. Bretcanu O, Chen Q, Misra SK, Boccaccini AR, Roy I, Verné E, Vitale-Brovarone C. Biodegradable polymer coated 45S5 Bioglass-derived glass-ceramic scaffolds for bone tissue engineering. *Glass Technol Eur J Glass Sci Technol A*. 2007;48:227–34.
21. Verrier S, Blaker JJ, Maquet V, Hench LL, Boccaccini AR. PDLA/Bioglass® composites for soft-tissue and hard-tissue engineering: an in vitro cell biology assessment. *Biomaterials*. 2004;25:3013–21. doi:[10.1016/j.biomaterials.2003.09.081](https://doi.org/10.1016/j.biomaterials.2003.09.081).
22. Hench LL. The story of Bioglass®. *J Mater Sci: Mater Med*. 2006;17:967–78. doi:[10.1007/s10856-006-0432-z](https://doi.org/10.1007/s10856-006-0432-z).
23. ASTM D638-08. Standard test method for tensile properties of plastics.
24. ISO 527-1:1993 standard. Plastics—determination of tensile properties.
25. ASTM F2150-07. Standard guide for characterization and testing of biomaterial scaffolds used in tissue-engineered medical products.
26. Zhang K, Wang Y, Hillmayer MA, Francis LF. Processing and properties of porous poly(-lactide)/bioactive glass composites. *Biomaterials*. 2004;25:2489–500. doi:[10.1016/j.biomaterials.2003.09.033](https://doi.org/10.1016/j.biomaterials.2003.09.033).
27. Vitale-Brovarone C, Verné E, Robiglio L, Martinasso G, Canuto RA, Muzio G. Biocompatible glass–ceramic materials for bone substitution. *J Mater Sci: Mater Med*. 2008;19:471–8. doi:[10.1007/s10856-006-0111-0](https://doi.org/10.1007/s10856-006-0111-0).
28. Karageorgiou V, Kaplan D. Porosity of 3D biomaterial scaffolds and osteogenesis. *Biomaterials*. 2005;26:5474–91. doi:[10.1016/j.biomaterials.2005.02.002](https://doi.org/10.1016/j.biomaterials.2005.02.002).
29. Kenesei P, Kadar Cs, Rajkovits Zs. The influence of cell-size distribution on the plastic deformation in metal foams. *J Lendvai Scr Mater*. 2004;50:295–300. doi:[10.1016/j.scriptamat.2003.09.046](https://doi.org/10.1016/j.scriptamat.2003.09.046).
30. Kokubo T, Takadama H. How useful is SBF in predicting in vivo bone bioactivity? *Biomaterials*. 2006;27:2907–15. doi:[10.1016/j.biomaterials.2006.01.017](https://doi.org/10.1016/j.biomaterials.2006.01.017).
31. Rezwani K, Chen QZ, Blaker JJ, Boccaccini AR. Biodegradable and bioactive porous polymer/inorganic composite scaffolds for bone tissue engineering. *Biomaterials*. 2006;27:3413–31. doi:[10.1016/j.biomaterials.2006.01.039](https://doi.org/10.1016/j.biomaterials.2006.01.039).
32. Jones J, Hench LL. Regeneration of trabecular bone using porous ceramics. *Curr Opin Solid State Mater Sci*. 2003;7:301–7. doi:[10.1016/j.cossms.2003.09.012](https://doi.org/10.1016/j.cossms.2003.09.012).
33. Bil M, Ryszkowska J, Roether JA, Bretcanu O, Boccaccini AR. Bioactivity of polyurethane-based scaffolds coated with Bioglass®. *Biomed Mater*. 2007;2:93–101. doi:[10.1088/1748-6041/2/2/006](https://doi.org/10.1088/1748-6041/2/2/006).
34. Ciardelli G, et al. Bioactive polyurethanes in clinical applications. *Polym Adv Technol*. 2006;17:786–9. doi:[10.1002/pat.781](https://doi.org/10.1002/pat.781).